Supporting Information

Armor-structured interconnected-porous membrane for corrosion-resistant and highly-permeable waste ammonium resource recycling

Dongqing Liu [†], Fuyun Yu [†], Lingling Zhong [†], Tao Zhang [†], Ying Xu [‡], Yingjie Qin [§], Jun Ma [†], Wei Wang [†,*] ,

[†] State Key Laboratory of Urban Water Resource and Environment (SKLUWRE), School of Environment, Harbin Institute of Technology, Harbin 150090, P. R. China

[‡] School of Ecology and Environment, Zhengzhou University, Zhengzhou 450000, China

[§] School of Chemical Engineering and Technology, Tianjin University, Tianjin 300072, China

* Corresponding authors, Email: wangweirs@hit.edu.cn

Number of Pages: 20

Number of Sections: 2

Number of Methods: 10

Number of Tables: 2

Number of Figures: 15

Section S1. Materials

Polyvinylidene fluoride (PVDF, Kynar® Hsv900, Mw~900,000) was purchased from Arkema Co., Ltd., China and Poly (vinylidene fluoride-co-hexafluoropropylene) (PVDF-HFP, Mw~400,000) was purchased from Sigma-Aldrich, China. Polytetrafluoroethylene (PTFE, DAIKIN® 10-120) nano-powders (120 nm) were obtained from Dongguan Xingwang Plastic Co. Ltd, China. N, N-dimethylacetamide (DMAc, 99.0%) and acetone (98%) were supplied from Shanghai Macklin Biochemical Co., Ltd and Tianjin Bohai Chemical Co., Ltd respectively. Ammonia chloride (NH_4Cl, 99.5%) and sodium hydroxide (NaOH, 96%) were purchased from Tianjin Kermel Chemical Reagent Co., Ltd. Sulfuric acid (H_2SO_4, 98%) and hydrochloric acid (HCl, 36%) were obtained from Xilong Scientific Co., Ltd. The commercial PTFE and PP membranes with different pore sizes were supplied from Haining Chuangwei Filter Equipment Technology CO., Ltd. All chemicals were analytical grade reagents without special emphasis and used as received without further purification.

Section S2. Characterizations

The surface morphology and structure of membranes were observed by field emission scanning electron microscope (FE-SEM, Sigma 500, ZEISS, Germany). The roughness of membranes containing different content of PTFE nano-powders was measured using atomic force microscope (AFM, Dimension FastScan, Bruker, Germany). The near-surface chemical compositions of NFMs before and after chemical treatment (soaking in alkaline solution (pH=12)) were analyzed by X-ray photoelectron

spectroscopy (XPS, ESCALAB 250Xi, USA). The mechanical properties of the membranes were tested by an electronic universal testing machine with a stretching speed of 50 mm/min provided by (Shenzhen) SUNS Technology Stock Co., Ltd. The zeta potential of the membrane surface was characterized by a streaming potential analyzer (SurPASS, Anton Paar GmbH, Austria) measured with a solution containing 1 mmol L^{-1} KCl. The pore size distribution and gas permeability were measured via a bubble pressure method supplied from (Beijing) Beishide Instrument Technology Co., Ltd. Contact angles (CAs) were investigated by a contact angle goniometer (KINO SL200B, USA) and each value was the average of five parallel tests. The liquid entry pressure of water (LEP_w) was measured using a homemade dead-end filtration device. Three-dimensional fluorescence spectrometer (F7000, Hitachi, Japan), which had an excitation wavelength of 200-450 nm, was qualitatively analyzed for fluorescent components in the solution. TOC/TN determinator (Multi N/C3100, Jena, Germany) and inductively coupled plasma-optical emission spectrometer (ICP-OES, PerkinElmer Optima 8300, USA) were used to analyze TN and TP in real wastewater respectively.

Method S1. Preparation of other comparative NFMs

A pristine PVDF solution was first prepared by dissolving 14 wt% PVDF in DMAc/acetone (70/30 wt%) solvent mixture with vigorous stirring at 80 ℃ for 4 h followed by overnight continuous stirring at room temperature. PH membranes with a spherical and spindle structure morphology was prepared by dissolving 14 wt% and 16 wt% PH in acetone/DMAc (70/30 wt%) mixed solvents, respectively. The electrospinning parameters were the same as those of armor-structured NFM (PTFE-PH/PVDF membrane). In particular, the humidity was controlled at 60±2% to ensure the morphology of the pristine PVDF nanofiber membranes. The pristine PVDF NFM (written as "PVDF NFM"), armor-structured NFM without PTFE doping (written as "PH/PVDF NFM"), and armor-structured NFM with different PTFE doping content (written as "α-PTFE-PH/PVDF NFM", where α denotes the mass fraction of PTFE) were prepared in same conditions to reduce the influence on the membrane structure by electrospinning.

Method S2. Optimization principle and method of recycling ammonia.

In the GMAR process, we mainly use the "control variate" method to discuss the effects of flow rate, pH of feed solution, and length of module on ammonia recovery. Firstly, the length of the module was controlled to be 3 cm and the pH of the feed solution was kept at 11, and the effect of different flow rates (35 mL/min, 60 mL/min, 85 mL/min, 115 mL/min) on ammonia recovery was investigated. Secondly, a module with a length of 3 cm was still selected and the flow rate of solution on both sides of

the membrane was controlled at 60 mL/min to test the influence of feed solution with different pH (9, 10, 11, 12) on ammonia recovery. Finally, the solution was cross-flowed at a flow rate of 60 mL/min and the pH of feed solution was 11, and the effect of different length modules (3 cm, 6 cm, 9 cm) on ammonia recovery was studied.

Method S3. Ammonia vapor flux (F_{NH_3}, g NH_3-N m^{-2} h^{-1}) and Overall mass transfer coefficient (Kov)

The ammonia vapor flux (F_{NH_3}, g NH_3-N m^{-2} h^{-1}) was calculated by measuring ammonium concentration in the absorbent side, which was expressed by Eq. (S1)

$$F_{NH_3-N} = \frac{c_a^t \cdot V_a}{1000 \times A \cdot t} \quad (S1)$$

where c_a^t is the concentration of NH_4^+-N in the absorbent solution at time t, mg L^{-1}; V_a is the volume of the absorbent solution, L; A is the effective membrane area, m^2; t is the reaction time, h.

The overall mass transfer coefficient (Kov) of IGM system was calculated by Eq. (S2)

$$K_{OV} = \frac{V_0}{At} ln\left(\frac{c_f^0}{c_f^t}\right) \quad (S2)$$

where K_{OV} is the overall mass transfer coefficient, m s^{-1}; V_0 is the volume of the feed solution, L. c_f^0 and c_f^t are the concentration of NH_4^+-N in the feed solution at the initial and t time, mg L^{-1}, respectively.

Method S4. Calculation of surface energy of armor-structured NFMs doped with different PTFE

The surface energy (γ_S) is composed of the dispersion (γ^D) and the polar bond (γ^P) forces, which can be calculated from the contact angles of two different solvents.[1] In this study, the surface energy of the fabricated membranes is measured by Owens-Wendt method, as follow Eq. (S3).

$$\gamma_L(1+\cos\theta) = 2\left(\sqrt{\gamma_{SG}^D \cdot \gamma_{LG}^D} + \sqrt{\gamma_{SG}^P \cdot \gamma_{LG}^P}\right) \quad \text{(S3)}$$

where γ_L is the interfacial tension of liquid. γ_{SG}^D and γ_{LG}^D are the dispersive component of solid and liquid, respectively; γ_{SG}^P and γ_{LG}^P are the polar component of solid and liquid, respectively; In this study, we analyze the surface energy by measuring the contact angle between water and diiodomethane on the membrane surface. The related parameters of the aforementioned solvents are presented in Table S2.

Method S5. Calculation of liquid entry pressure

The liquid entry pressure of water (LEPw) is usually considered as the minimum transmembrane pressure for liquid water to overcome the hydrophobic surface and enter the membrane pore, which is an important criterion to measure the resistance of the membrane to wetting.[2] The LEP_w of membrane can be calculated by Young-Laplace equation as follow Eq. (S4)

$$LEP_w = -\frac{2B\gamma cos\theta}{d_{max}} \quad \text{(S4)}$$

where B is a pore geometry coefficient; γ is the liquid surface tension, γ_{water}=72.58 mN/m; θ is the water contact angle on the membrane surface, °; d_{max} is the maximum

membrane pore size, μm.

Method S6. Normalized calculation of TAN

$$c_{N,TAN} = c_a^t \frac{V_t}{V_0} \quad (S5)$$

where $c_{N,TAN}$ is the normalized concentration of NH_4^+-N in the absorbent solution, mg L^{-1}; c_a^t is the concentration of NH_4^+-N in the absorbent solution at time t, mg L^{-1}; V_t is the volume of the initial absorbent solution, L; V_0 is the volume of the feed solution, L.

Method S7. Dissociation equilibrium equations

Total ammonia nitrogen mainly exists in solution in the form of free ammonia (NH_3) and ammonium salt (NH_4^+).[3] The dissociation equilibrium of ammonia in an aqueous solution can be described by Eq. (S6-9)

$$NH_3 + H_2O \rightleftharpoons NH_4^+ + OH^- \quad (S6)$$

$$K_b = \frac{[NH_4^+][OH^-]}{[NH_3]} \quad (S7)$$

$$\alpha_{NH_3} = \frac{[NH_3]}{[NH_3] + [NH_4^+]} = \frac{[OH^-]}{K_b + [OH^-]} \quad (S8)$$

$$\alpha_{NH_4^+} = \frac{[NH_4^+]}{[NH_3] + [NH_4^+]} = \frac{K_b}{K_b + [OH^-]} \quad (S9)$$

where $[NH_4^+]$, $[NH_3]$, and $[OH^-]$ are the equilibrium concentrations of ammonium, ammonia, and hydroxyl, respectively. α is the concentration distribution fraction of different components. K_b is the dissociation equilibrium constant for ammonia, which is calculated by Eq. (S10).

146 $$\frac{K_b}{K_W} = e^{(6344/(273+T))} \quad (S10)$$

147 where Kw is the ionization product constant of water, which is related to temperature.

148

149

150 **Method S8.** Calculation of porosity

151 The porosity for commercial and fabricated membranes was calculated using
152 gravimetric method as follow Eq. (S11). Firstly, the dry weight of the 4cm×2cm
153 membrane was weighed as W_1; whereafter, the membrane was saturated in isopropyl
154 alcohol/water (50/50 vol%) for 24h, and the liquid on the surface of the membrane was
155 wiped with filter paper and weighed as W_2.[4]

156 $$\varepsilon = \frac{(W_2 - W_1)/D_{i/w}}{(W_2 - W_1)/D_{i/w} + W_1/D_p}$$

157 (S11)

158 where W_1 and W_2 are the dry and wet weights of membranes, g, respectively; $D_{i/w}$
159 represents the density of isopropyl alcohol/water solution, $D_{i/w}$=0.8925 g/cm^3; D_p is the
160 density of polymers, which is calculated by the weighted average of polymer content in
161 the fabricated membranes.

162

163 **Method S9.** Analysis of Fluorescence Spectrum

164 To analyze the anti-wettability performance of the armor-structured NFM, the
165 organic compounds in the solution on both sides of the membrane were characterized
166 by fluorescence excitation-emission matrix spectrum (EEM). The EEM spectrums of

the samples were analyzed by PARAFAC analysis. The fluorescence intensities were detected at excitation (ex) wavelengths of 200-450 nm at 5 nm intervals, within the range of emission (em) wavelengths from 250 to 550 nm at 1 nm intervals. The EEM spectrum of Milli-Q water was deducted from each sample to remove Raman scatter peaks. The EEM components monitored in this study were region Ⅰ (tyrosine-like, ex 200-250 nm, and em 250-330 nm), region Ⅱ (tryptophan-like, ex 200-250 nm, and em 330-380 nm), region Ⅲ (fulvic acid-like, ex 200-250 nm, and em 380-500 nm), region Ⅳ (soluble microbial byproduct substances, ex 250-340 nm, and em 300-380 nm), and Ⅴ (humic acid-like, ex 250-400 nm, and em 380-500 nm).[5, 6]

Method S10. Energy consumption analysis

Energy consumption analysis of GMAR system based on ammonia flux,

$$E_{con} = \frac{W}{J_{NH_3}} \quad \text{(S12)}$$

where E_{con} is the energy consumption, kWh $kg^{-1}N$; W is the electrical energy input to the system, kW h; J_{NH_3} is the ammonia flux in a certain time period, kgN.

184 Table S1. The first stage aerobic digestion effluent quality of actual hoggery

185 (Harbin, China)

Parameters	pH	CODcr	NH_4^+-N	TN	TP
Value	8.46 (±0.02)	454(±38) mg/L	945(±48) mg/L	995(±38) mg/L	10(±1) mg/L

186

187 Table S2. Surface energy of solvents used in current study

Solvents	Surface tension (γ_L, mN/m)	Dispersive component (γ_L^D, mN/m)	Polar component (γ_L^P, mN/m)
Water	72.8	21.8	51
Diiodomethane	50.8	50.8	0

188

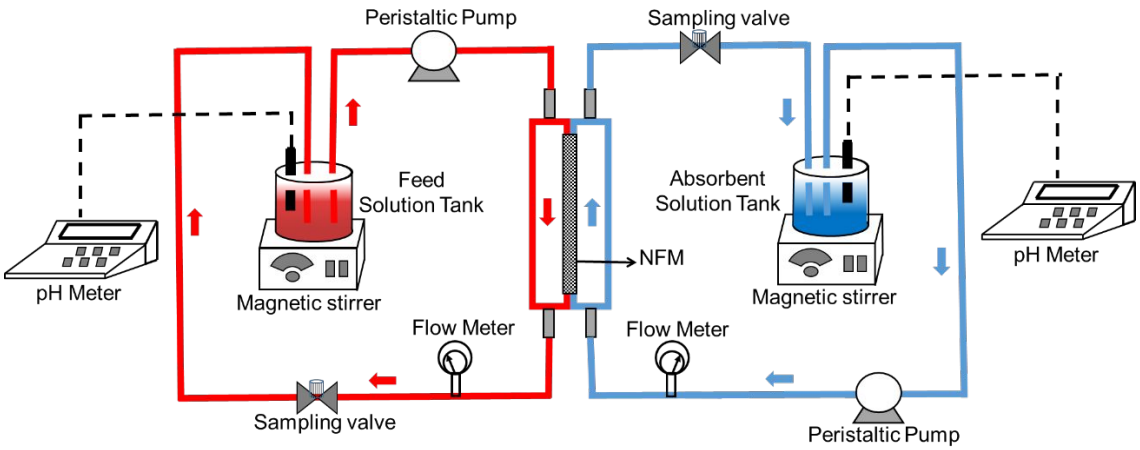

189

190 **Figure S1.** Experimental setup for lab-scale isothermal gas-permeable membrane

191 system.

192

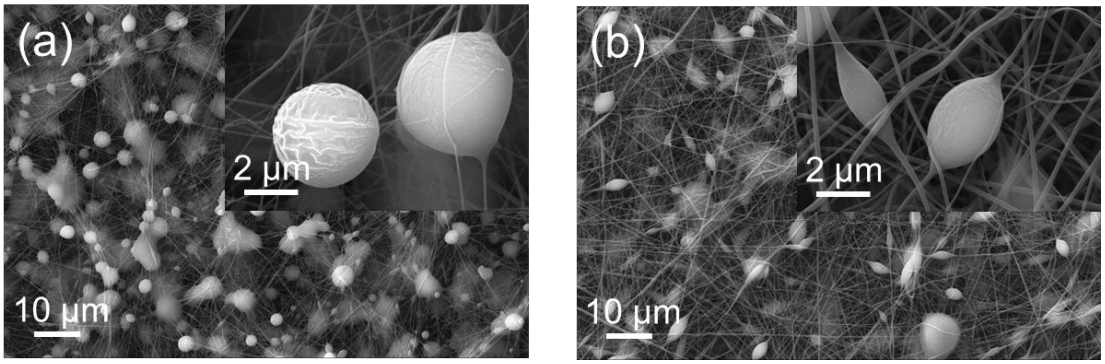

193

194 **Figure S2.** SEM images of PH membranes with different mass fraction (a) 14 wt% PH

195 and (b) 16 wt%PH.

196

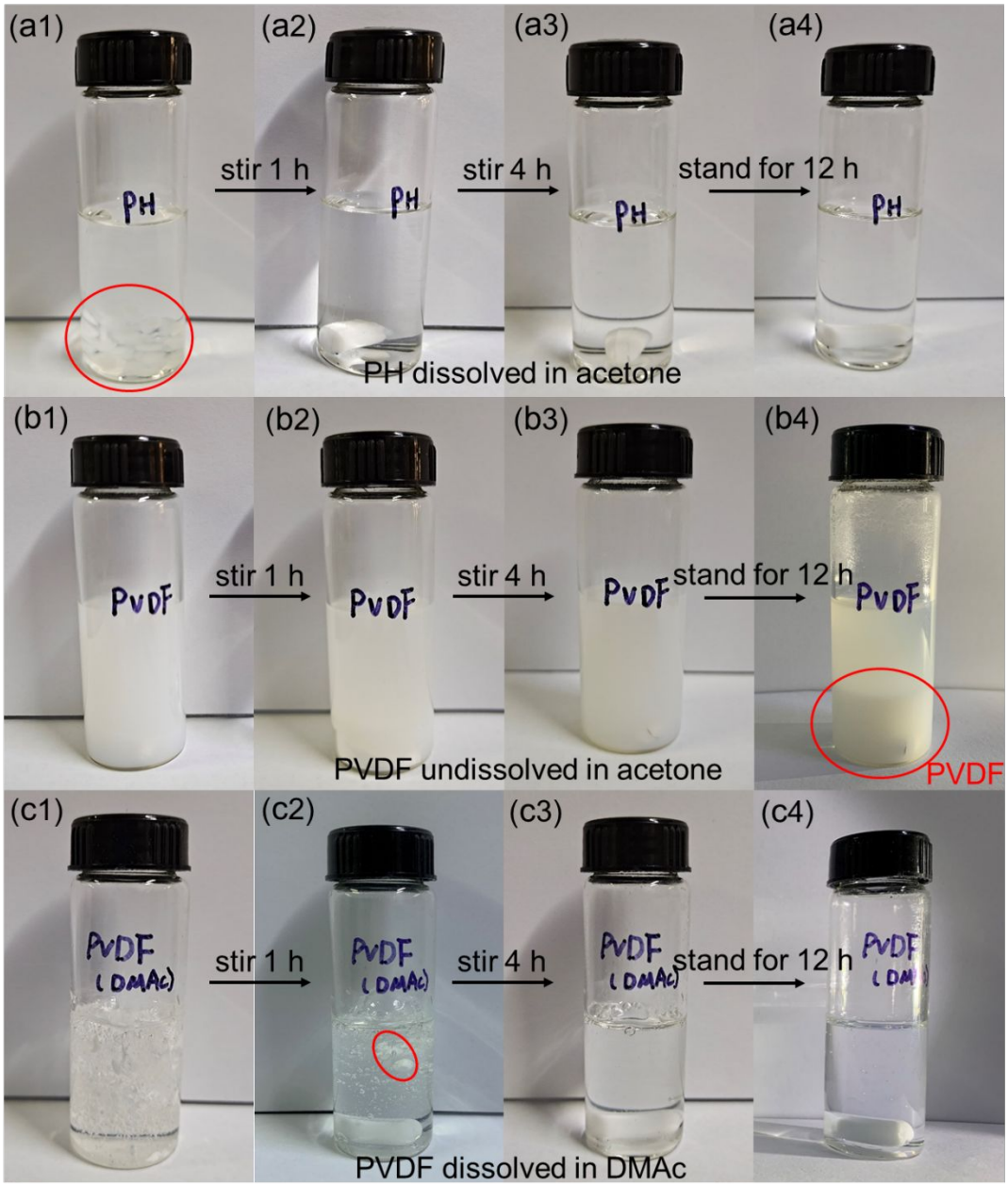

197

198 **Figure S3.** (a) Solubility of PH in acetone; (b) Solubility of PVDF in acetone; (c)

199 Solubility of PVDF in DMAc.

200

201

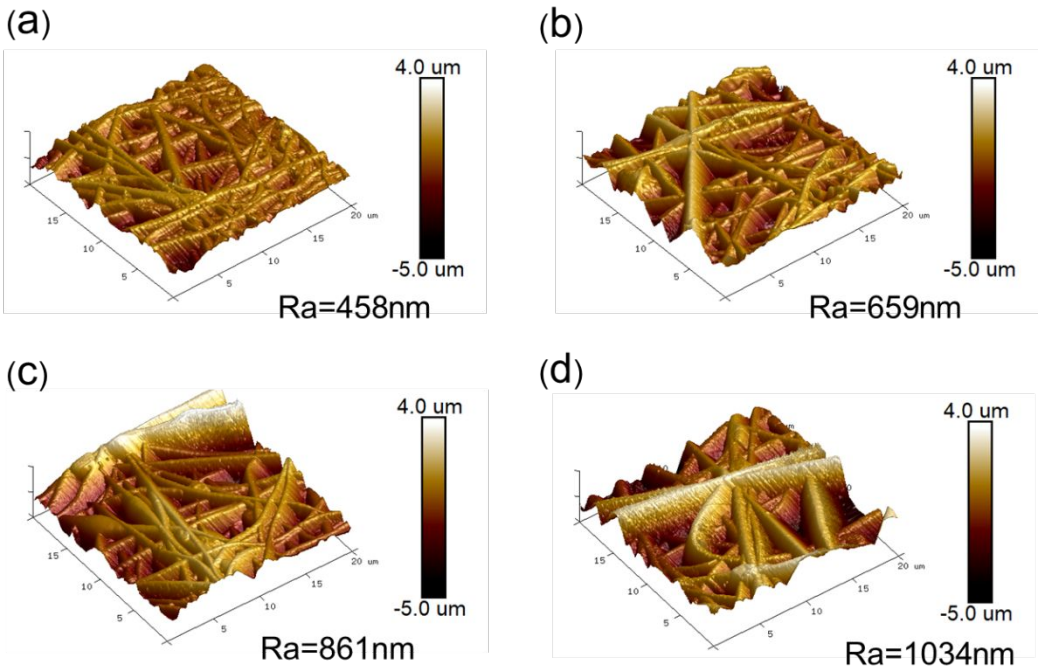

202

203 **Figure S4.** AFM images of armor-structured NFMs. (a) 0 wt%-PTFE-PH/PVDF NFM

204 (PVDF/PH NFM), (c) 2.5 wt%-PTFE-PH/PVDF NFM, (d) 5.0 wt%-PTFE-PH/PVDF

205 NFM, and (e) 10.0 wt%-PTFE-PH/PVDF NFM

206

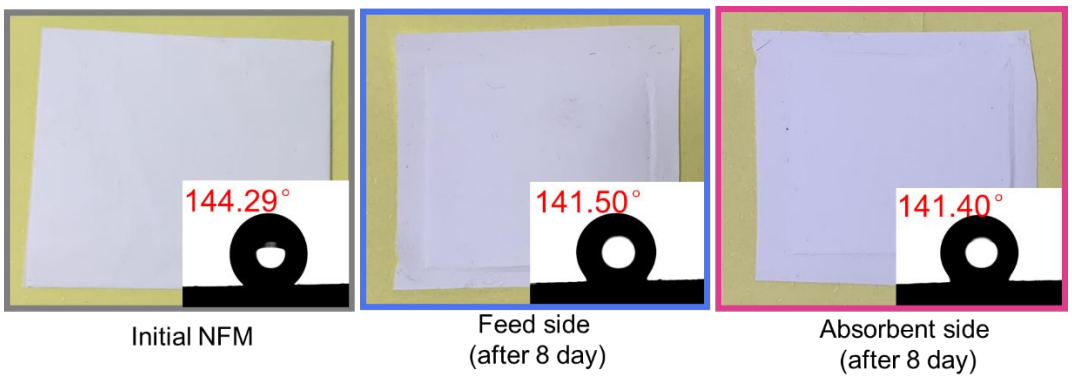

207

208 **Figure S5.** Water Contact Angles on both sides of armor-structured membrane before

209 and after 8-day intermittent operation

210

211

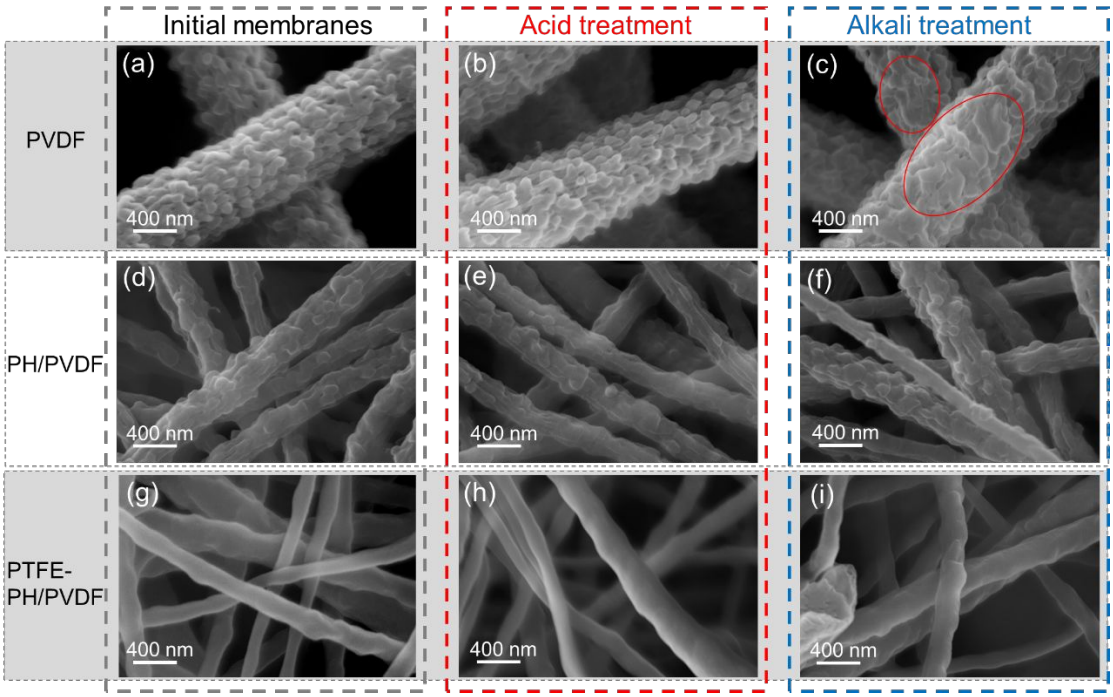

Figure S6. SEM of (a) PVDF NFM, (b) PVDF NFM treated with acid for 3 days, (c) PVDF NFM treated with alkali for 3 days, (d) Armor-structured NFM without PTFE doping (PH/PVDF NFM), (e) PH/PVDF NFM treated with acid for 3 days, (f) PH/PVDF NFM treated with alkali for 3 days, (g) Armor-structured NFM with PTFE doping (PTFE-PH/PVDF NFM), (h) PTFE-PH/PVDF NFM treated with acid for 3 days, (i) PTFE-PH/PVDF NFM treated with alkali for 3 days.

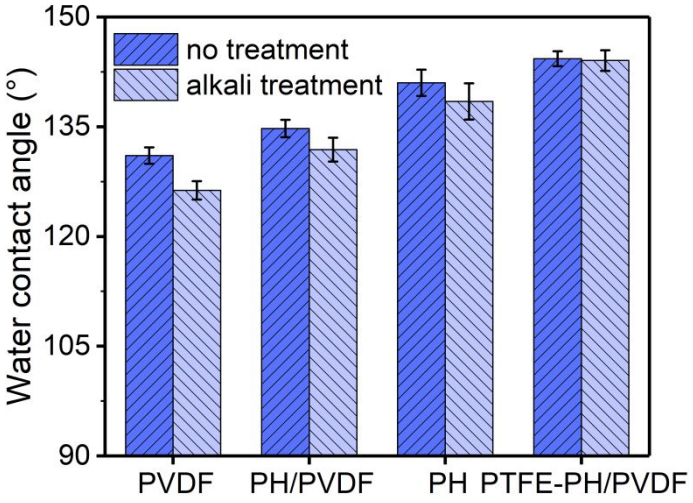

Figure S7. The change of Water Contact Angle of different nanofibrous membranes before and after alkali treatment.

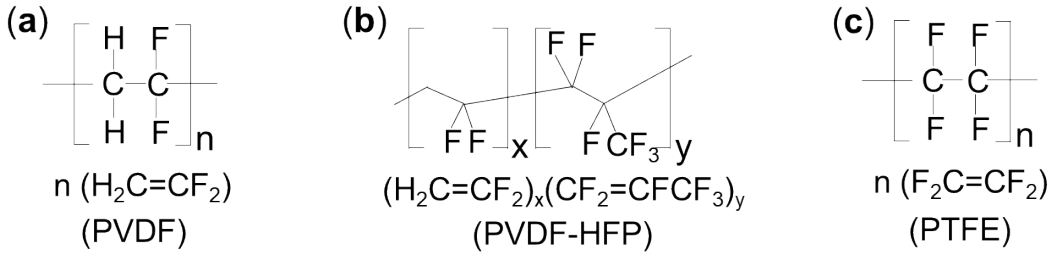

Figure S8. Molecular structure of PVDF (a), PVDF-HFP (b), and PTFE (c).

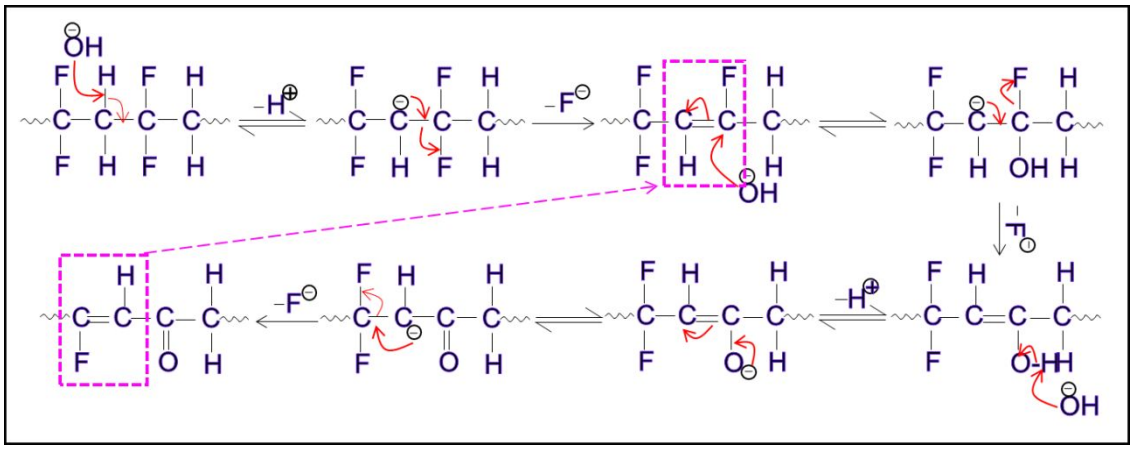

Figure S9. Defluorination mechanism of PVDF in alkaline condition.

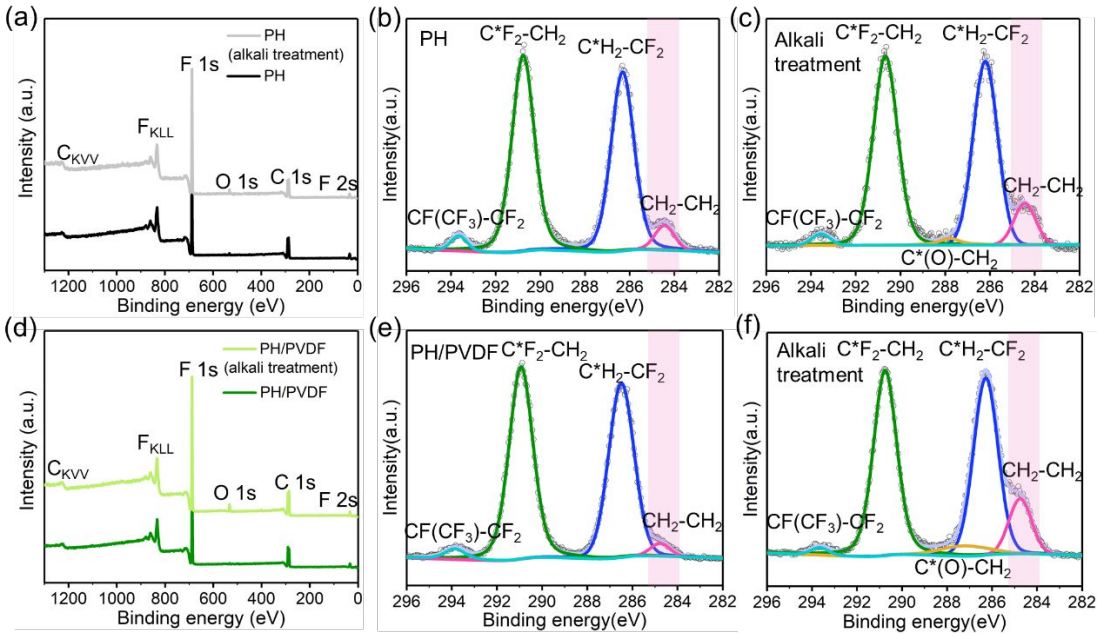

231

232 **Figure S10.** Element component analysis of the surface of PH (a) and PH/PVDF (d)

233 NFM before and after alkali treatment; C 1s XPS spectra of PH NFM before (b) and

234 after (c) alkali treatment; C 1s XPS spectra of PH/PVDF NFM before (e) and after (f)

235 alkali treatment.

236

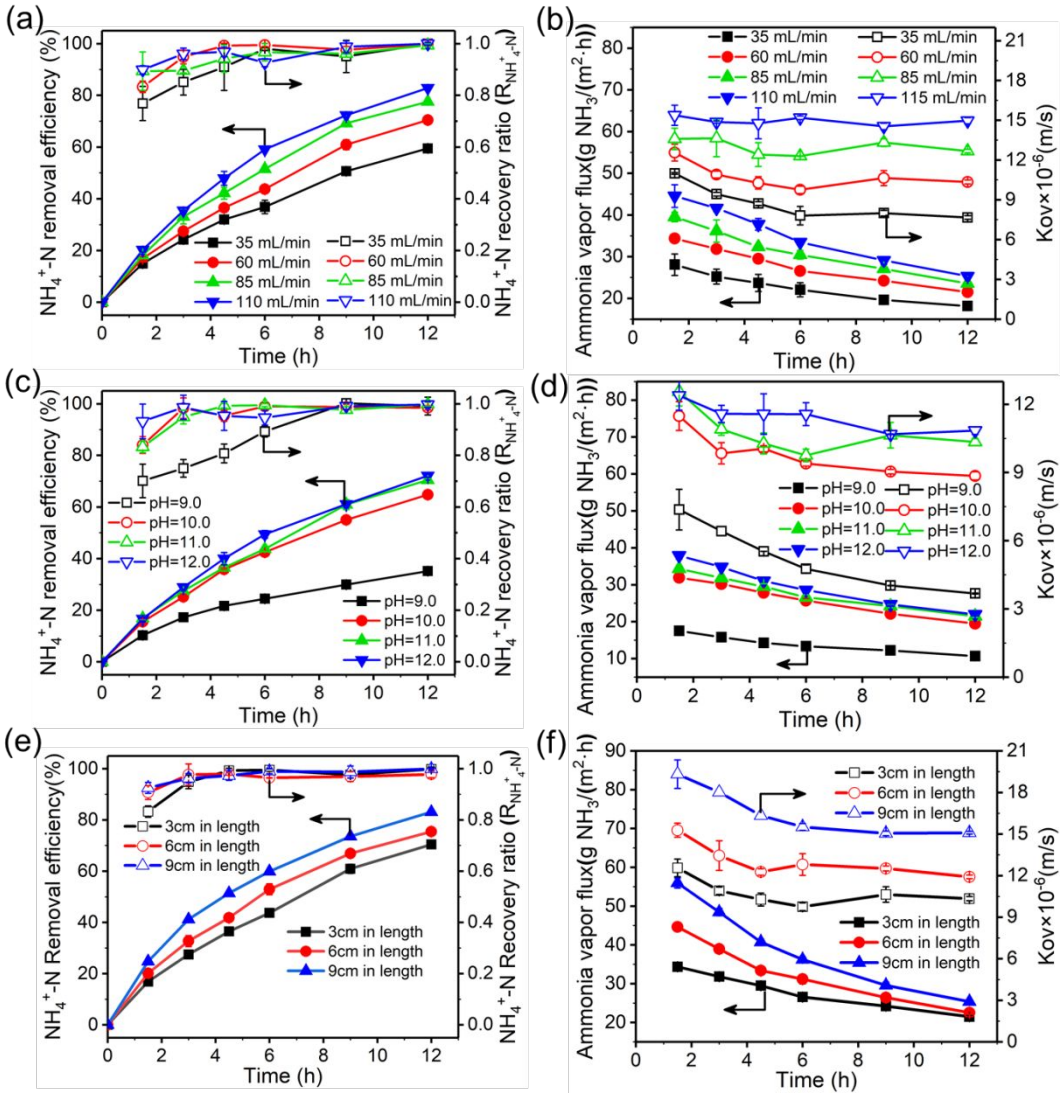

237

238 **Figure S11.** Effect of different parameters on GMAR process.NH_4^+-N removal

239 efficiency and recovery ratio versus time at different flow velocity (a), pH (c), and

240 module size (e); Ammonia flux and Kov versus time at different flow velocity (b), pH

241 (d), and module size (f).

242

243

244

245

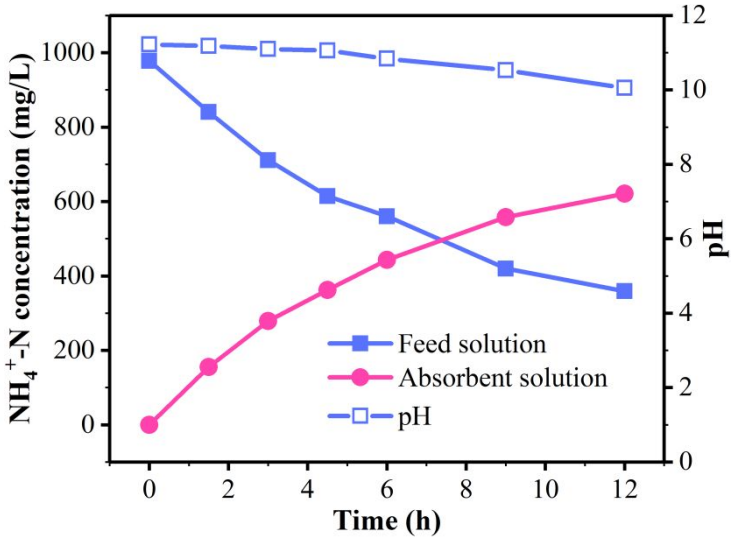

246

247 **Figure S12.** NH_4^+-N recovery performance of PTFE with pore size of 1 μm.

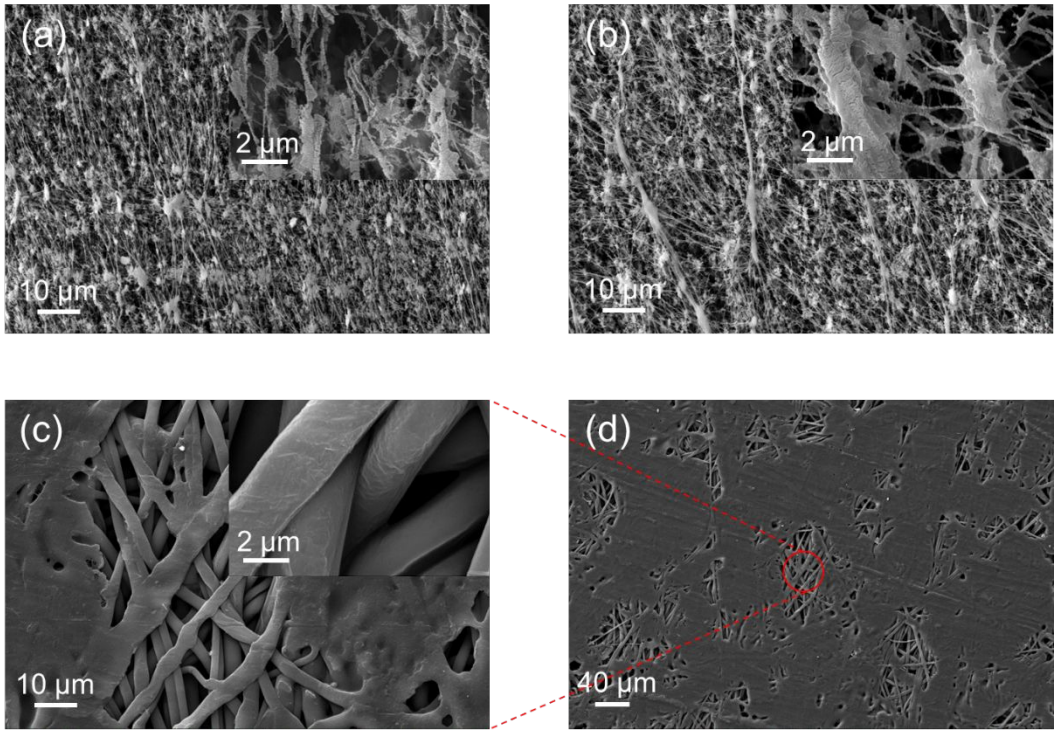

248

249 Figure S13. SEM images of commercial PTFE membranes with different pore size of

250 (a) 0.45 μm and (b) 1.0 μm, respectively, (c) and (d) SEM images of commercial PP

251 membranes.

252

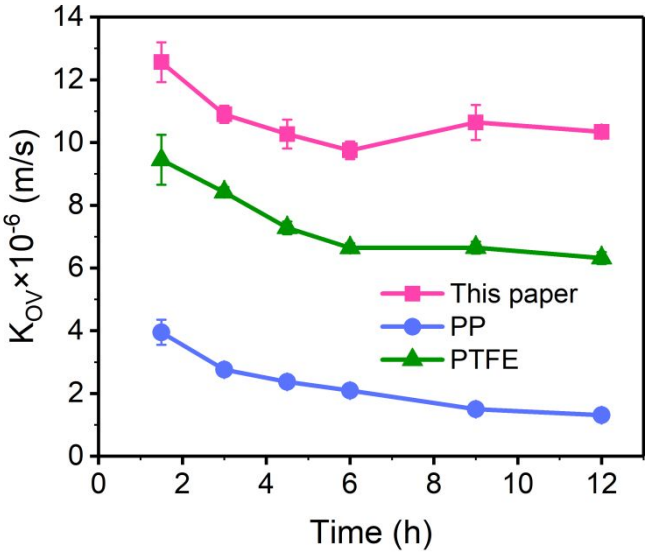

Figure S14. The overall mass transfer coefficient of different membranes.

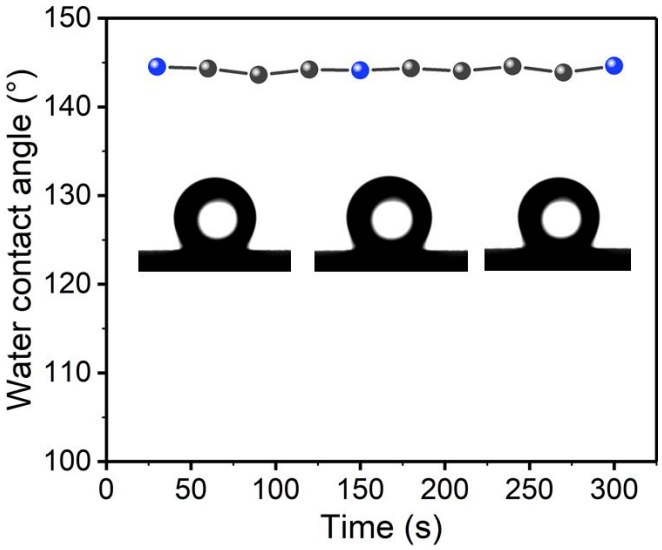

Figure S15. The hoggery wastewater contact angle of armor-structured NFM.

REFERENCE

1. Zhong, L.; An, L.; Han, Y.; Zhu, Z.; Liu, D.; Liu, D.; Zuo, D.; Wang, W.; Ma, J. In Situ Three-Dimensional Welded Nanofibrous Membranes for Robust Membrane Distillation of Concentrated Seawater. *Environ. Sci. Technol.* **2021,** *55*, (16), 11308-11317.

2. Zhu, Z.; Liu, Y.; Hou, H.; Shi, W.; Qu, F.; Cui, F.; Wang, W. Dual-Bioinspired Design for Constructing Membranes with Superhydrophobicity for Direct Contact Membrane Distillation. *Environ. Sci. Technol.* **2018,** *52*, (5), 3027-3036.

3. He, L.; Wang, Y.; Zhou, T.; Zhao, Y. Enhanced ammonia resource recovery from wastewater using a novel flat sheet gas-permeable membrane. *Chem. Eng. J.* **2020,** *400*.

4. Deka, B. J.; Lee, E.-J.; Guo, J.; Kharraz, J.; An, A. K. Electrospun Nanofiber Membranes Incorporating PDMS-Aerogel Superhydrophobic Coating with Enhanced Flux and Improved Antiwettability in Membrane Distillation. *Environ. Sci. Technol.* **2019,** *53*, (9), 4948-4958.

5. Murphy, K. R.; Butler, K. D.; Spencer, R. G. M.; Stedmon, C. A.; Boehme, J. R.; Aiken, G. R. Measurement of Dissolved Organic Matter Fluorescence in Aquatic Environments: An Interlaboratory Comparison. *Environ. Sci. Technol.* **2010,** *44*, (24), 9405-9412.

6. Chen, W.; Westerhoff, P.; Leenheer, J. A.; Booksh, K. Fluorescence excitation - Emission matrix regional integration to quantify spectra for dissolved organic matter. *Environ. Sci. Technol.* **2003,** *37*, (24), 5701-5710.